

Nanobubble Trouble on Gold Surfaces

Maria Holmberg,^{*,†,‡} Anders Kühle,[†] Jørgen Garnæs,[†] Knud A. Mørch,[§] and Anja Boisen[‡]

Danish Fundamental Metrology (DFM), Matematiktorvet 307, DK-2800 Kgs. Lyngby, Denmark, and Mikroelektronik Centret (MIC), Technical University of Denmark (DTU), Building 345 east, DK-2800 Kgs. Lyngby, Denmark, and Department of Physics and the Quantum Protein Center, Technical University of Denmark (DTU), Building 309, DK-2800 Kgs. Lyngby, Denmark

Received July 12, 2003. In Final Form: September 9, 2003

When analyzing surfaces related to biosensors with in situ atomic force microscopy (AFM), the existence of nanobubbles called for our attention. The bubbles seem to form spontaneously when gold surfaces are immersed in clean water and are probably a general phenomenon at water–solid interfaces. Besides from giving rise to undesired effects in, for example, biosensors, nanobubbles can also cause artifacts in AFM imaging. We have observed nanobubbles on unmodified gold surfaces, immersed in clean water, using standard silicon AFM probes. Nanobubbles can be made to disappear from contact mode AFM images and then to reappear by changing the scanning force. By combining contact mode AFM imaging and local force measurements, the interaction between the nanobubbles and the probe can be analyzed and give information about the characteristics of nanobubbles. A model of the forces between the AFM probe tip and the nanobubble indicates that a small tip cone angle and a relatively hydrophilic tip surface makes it possible to image nanobubbles with contact mode AFM even though the tip has penetrated the surface of the bubble.

Introduction

For the last couple of years, it has been suggested that the long-range attractive force, also called the “hydrophobic interaction”, between hydrophobic surfaces in a liquid environment is caused by nanobubbles.^{1–10} Both theoretical^{1–4} and experimental^{5–10} work arguing for the existence of nanobubbles on surfaces have been published. Force measurements have been published to demonstrate the presence of nanobubbles indirectly, and tapping mode atomic force microscopy (AFM) imaging has further supported it. In those previous experiments, surfaces and probes have been modified to be highly hydrophobic. Imaging has been made in the tapping mode with standard AFM probes (radius around 10–20 nm), while force measurements have been performed with AFM probes with highly hydrophobic spheres (radius around 5–10 μm) attached to the tip apex.^{5,7}

During AFM experiments in liquid on surfaces related to cantilever-based biosensors,¹¹ we became aware of the

possible existence of nanobubbles on unmodified gold surfaces. In the cantilever-based biosensor, molecules are immobilized on a gold surface, and the quality of the molecular layer influences the quality of the biosensor. If nanobubbles are present on the gold surface during immobilization, they could lead to a nonhomogeneous molecular layer and, thus, have a significant effect on the characteristics of the sensor. Furthermore, during AFM imaging the interactions between the probe tip and the nanobubbles cause undesired features in images and makes them difficult to interpret. Our results suggest that the existence of nanobubbles is possible on unmodified surfaces and occur in systems in which they have not previously been considered.

In this paper, we present results from contact mode imaging and local force measurements performed on gold surfaces immersed in clean¹² water. To our knowledge, these are the first contact mode AFM images of nanobubbles published. The combination of contact mode imaging and local force measurements provides possibilities to investigate the interaction between the probe tip and the nanobubbles in detail. Others have published detailed theoretical discussions on force measurements.^{7,10,13} In this paper, we limit ourselves to an introductory analysis of force curves obtained during our measurements to emphasize the possibilities in combining contact mode imaging and local force measurements.

Experimental Section

All experiments presented were performed in clean water with a commercial AFM microscope.¹⁴ Standard contact mode silicon AFM probes with nominal force constants between 0.03 and 0.08 nN/nm and nominal resonant frequencies between 10 and 20 kHz in air were used. The height of the probe tip is around 15–

* Author to whom correspondence should be addressed. E-mail: mh@dfm.dtu.dk.

[†] Danish Fundamental Metrology.

[‡] Mikroelektronik Centret, Technical University of Denmark.

[§] Department of Physics and the Quantum Protein Center, Technical University of Denmark.

(1) Attard, P. *Langmuir* **1996**, *12*, 1693–1695.

(2) Attard, P.; Moody, M. P.; Tyrrell, J. W. G. *Physica A* **2002**, *314*, 696–705.

(3) Attard, P. *Langmuir* **2000**, *16*, 4455–4466.

(4) Mørch, K. A. *J. Fluids Eng.* **2000**, *122*, 494–498.

(5) Tyrrell, J. W. G.; Attard, P. *Phys. Rev. Lett.* **2001**, *87*, 176104(1)–176104(4).

(6) Carambassis, A.; Jonker, L. C.; Attard, P.; Rutland, M. W. *Phys. Rev. Lett.* **1998**, *80*, 5357–5360.

(7) Tyrrell, J. W. G.; Attard, P. *Langmuir* **2002**, *18*, 160–167.

(8) Ishida, N.; Inoue, T.; Miyahara, M.; Higashitani, K. *Langmuir* **2000**, *16*, 6377–6380.

(9) Lou, S.-T.; Ouyang, Z.-Q.; Zhang, Y.; Li, X.-J.; Hu, J.; Li, M.-Q.; Yang, F.-J. *J. Vac. Sci. Technol., B* **2000**, *18*, 2573–2575.

(10) Christenson, H. K.; Claesson, P. M. *Adv. Colloid Interface Sci.* **2001**, *91*, 391–436.

(11) Marie, R.; Jensenius, H.; Thaysen, J.; Christensen, C. B. V.; Boisen, A. *Ultramicroscopy* **2002**, *91*, 29–36.

(12) Milli-Q water, Millipore A/S, Odinsvej 9 St., 2600 Glostrup, Denmark.

(13) Craig, V. S. J.; Ninham, B. W.; Pashley, R. M. *Langmuir* **1999**, *15*, 1562–1569.

(14) Nanoscope MultiMode III Scanning Probe Microscope, Digital Instruments, U.S.A.

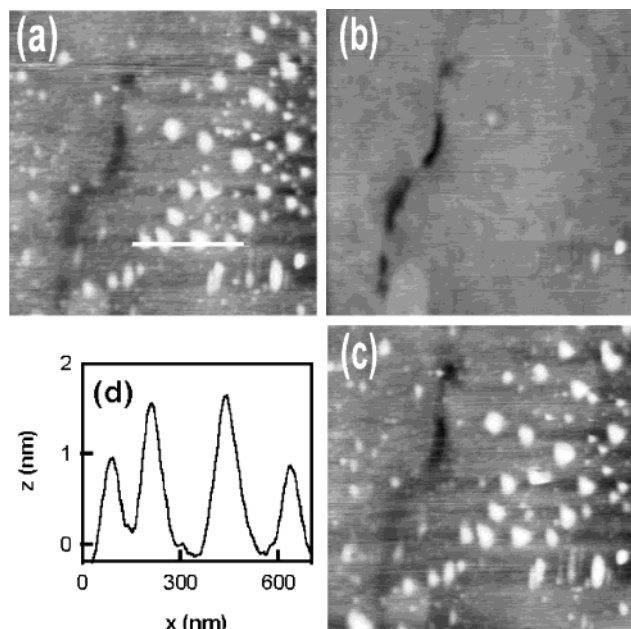


Figure 1. AFM image of a $2\ \mu\text{m} \times 2\ \mu\text{m}$ area on a gold surface immersed in clean water, which has been scanned in contact mode with a low scanning force (a), with a slightly higher scanning force (b), and again with a low scanning force (c). The brighter areas in parts a and c are interpreted to be nanobubbles. In part b, the same areas have a low, dark contrast. Part d shows a profile of four nanobubbles in part a. It can be seen that an apparent height around 1–1.5 nm can be measured when bubbles with diameters around 100 nm are imaged.

$20\ \mu\text{m}$, and the nominal curvature radius is 10 nm or less.¹⁵ Gold surfaces with ultraflat plateaus (up to $\sim 500\ \text{nm} \times 500\ \text{nm}$ in area) were obtained by evaporating gold onto mica substrates.¹⁶ The mica substrates were pre-annealed for at least 24 h at $512\ ^\circ\text{C}$ before 150-nm gold was evaporated with a low evaporation rate. After evaporation, the substrates were postannealed for 1 h at $512\ ^\circ\text{C}$. Both the silicon AFM probes and the gold surfaces were exposed to an ambient atmosphere during storage but were not intentionally chemically modified in any way. The gold surfaces were typically imaged with a scan speed of $8\ \mu\text{m}/\text{s}$ along the fast scan axis. Data analysis was performed using the software package SPIP.¹⁷

Results and Discussion

We have obtained tapping mode AFM images of nanobubbles on unmodified gold surfaces comparable to those published by others,^{7–9} and these are, therefore, not shown. On tapping mode images, the size and position of brighter areas in the topographical AFM image correspond to change in the phase AFM image, and we interpret the brighter areas as nanobubbles. A change in the phase image indicates a change in character of the material on the sample surface with which the scanning probe is interacting. To further confirm the existence of nanobubbles and to investigate their properties, we have, in addition, performed contact mode AFM experiments on the gold surfaces.

Figure 1 shows a series of contact mode images of the same $2\ \mu\text{m} \times 2\ \mu\text{m}$ area on a gold surface obtained at approximately 5-min intervals. Both before and after obtaining the images, force curves were recorded to estimate the scanning force used during measurements. Figure 1a is an image obtained where the setpoint has

been adjusted to give the lowest possible scanning force without losing contact with the sample. Between the recording of part a and that of part b of Figure 1, the scanning force has been increased a few nano-Newtons, and between the recording of part b and that of part c of Figure 1, the scanning force has been reduced to approximately the same value as that used in Figure 1a. The dark, longish area on the images is a groove in the gold surface, which is formed naturally during the evaporation of gold onto mica.

As can be seen in Figure 1a, when the lower scanning force is used, bright domains of varying size can be observed on the image, and we interpret these structures as nanobubbles. When the scanning force is increased, almost all of the bright domains either disappear or are transformed into smaller and darker areas (Figure 1b). When the scanning force is reduced again, the bright domains reappear essentially with the same size and at the same positions as those in Figure 1a. The fact that the bright structures can be made to disappear and then reappear at the same spots on the gold surface by changing the scanning force supports the assumption that the bright structures are nanobubbles. If they were particles, they would typically be swept away from the scanned area and aggregate at the edges of the area. However, Steitz et al.¹⁸ have recently shown that nanobubbles can be coalesced into a bigger bubble through manipulation with an AFM tip, and the ability to manipulate nanobubbles with an AFM tip is related to the surface material and AFM probe involved. It is not clear why the bubbles in Figure 1 are stable in position on the gold surface because no underlying structure, to which the bubbles could be connected, can be observed on the images. One may speculate that adsorbents from the ambient, or characteristics of the surface not observable in the experiments, can play a role.

In Figure 1a,c, nanobubbles with a diameter ~ 50 – $130\ \text{nm}$ have a height ~ 0.4 – $1.5\ \text{nm}$ (see Figure 1d). In other contact mode measurements, where a lower scanning force was used, we observed that bubbles with a diameter of $\sim 100\ \text{nm}$ had a height of $\sim 5\ \text{nm}$. When bubbles with diameters in this range were imaged in the tapping mode, the apparent height was $\sim 6\ \text{nm}$.

In force curves obtained before and after the recording of Figure 1a, the baseline has drifted approximately 140 nm. The tendency of baseline drift becomes smaller during the recording of Figure 1b,c. When comparing the estimated forces used in obtaining Figure 1 and the measured forces from other AFM experiments on gold surfaces with nanobubbles, where the baseline drift has been negligible, we can conclude that the force used during the imaging of nanobubbles as bright structures has been ~ 0.3 – $0.5\ \text{nN}$. The reason for the abnormal drift in this particular measurement is unknown, but could be explained by thermal drift and influence from macroscopic bubbles, which sometimes gather around the cantilever substrate and offset the deflection monitoring system.

Even though it has not been possible to determine the exact magnitude of the scanning force used during the recording of the images in Figure 1, it is clear that depending on the scanning force used, nanobubbles with approximately the same dimensions can be represented with different diameters and heights in AFM images. We suggest that it is possible to image nanobubbles with a reduced diameter and height by penetrating the surface of the bubble with the AFM probe tip, where an equilibrium

(15) Silicon ULTRASHARP Cantilever, CSC12, MikroMasch Scanning Probe Microscope TIPS, Estonia.

(16) Holmberg, M.; Kühle, A.; Garnæs, J.; Boisen, A. *Ultramicroscopy* **2003**, *97*, 257–261.

(17) SPIP, version 3.0. Image Metrology ApS: Denmark, 2003.

(18) Steitz, R.; Gutgerlet, T.; Hauss, T.; Klösgen, B.; Krastev, R.; Schemmel, S.; Simonsen, A. C.; Findenegg, G. H. *Langmuir* **2003**, *19*, 2409–2418.

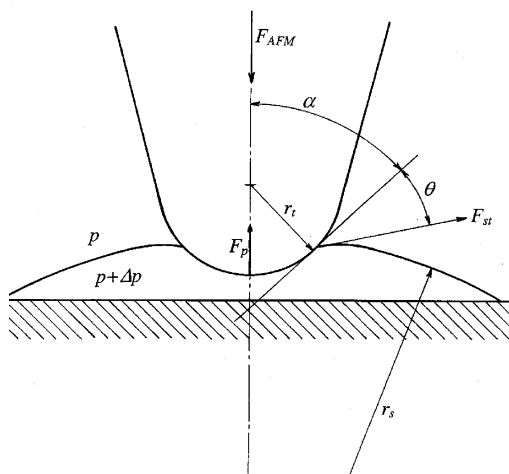


Figure 2. Schematic picture of the AFM probe tip and nanobubble (not to scale) during interaction in AFM contact mode imaging.

between the forces involved in the scanning of the surface can be obtained. Our experimental results combined with the simple model in Figure 2 indicate that this is possible when the tip cone angle of the AFM probe is small and when the tip is hydrophilic (contact angle less than $\sim 90^\circ$).

The equation to be solved is

$$F_{\text{AFM}} - F_p - F_{\text{st}} = 0 \quad (1)$$

where F_{AFM} is the vertical force applied by the AFM probe tip on the bubble interface, F_p is the force caused by the pressure difference across the bubble wall over the area where the tip and the bubble interact, and F_{st} is the vertical component of the force caused by the surface tension along the line where the tip and the bubble interact.

Equation 1 can be written as

$$F_{\text{AFM}} - \Delta p \pi (r_t \cos \alpha)^2 - 2\pi \gamma r_t \cos \alpha \cos(\alpha + \theta) = 0 \quad (2)$$

where Δp is the pressure difference between the inside and the outside of the nanobubble, r_t is the curvature radius of the tip apex, α is the angle between the normal of the tip and the tangent to the circle, which approximates the tip shape at the apex, along the line where the bubble and water meet, γ is the surface tension, and θ is the contact angle (see Figure 2).

During imaging, F_{AFM} is greater than 0 ($F_{\text{AFM}} \geq 0$). Applying this condition to eq 2 yields

$$\Delta p \geq -\gamma \frac{2 \cos(\alpha + \theta)}{r_t \cos \alpha} \quad (3)$$

This can be combined with the Young–Laplace equation¹⁹ for a bubble

$$\Delta p = 2\gamma/r_s \quad (4)$$

where r_s is the radius of a sphere with the same curvature as the nanobubble. The result is

$$\frac{r_t}{r_s} \geq -\frac{\cos(\alpha + \theta)}{\cos \alpha} \quad (5)$$

Estimating r_t to 10 nm and r_s to 1 μm , one finds that $\alpha + \theta$ should not exceed 90° to achieve an equilibrium. Thus, according to these calculations, by using a small tip

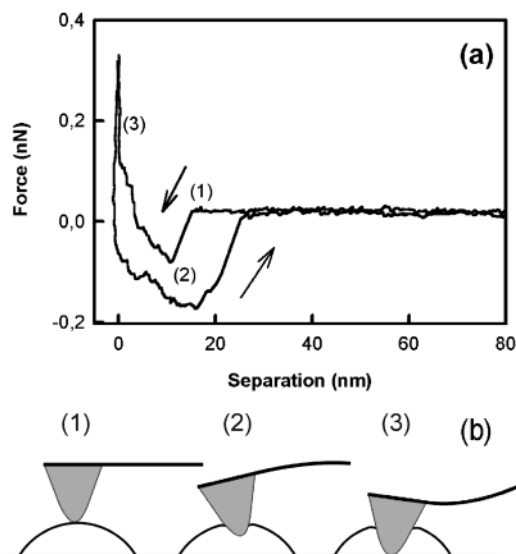


Figure 3. Typical force curve obtained in an area containing nanobubbles with diameters around 250 nm or smaller is shown (a). The force curve is believed to represent an interaction between a single nanobubble (diameter around 150 nm) and the probe tip. There is a “snap-in” at a separation of 12–15 nm in the approaching curve and a “snap-out” at a separation of 15–20 nm in the retraction curve. In part b, the interaction between the tip and the bubble is shown (not to scale) just before “snap-in” (1), just after “snap-in” (2), and during hard-wall contact (3).

angle and a relatively hydrophilic tip, nanobubbles can be imaged in the AFM contact mode with the tip penetrating the bubble surface. To estimate the contact angle between the tip and the clean water, contact angle measurements have been performed on standard silicon wafers with native oxide in clean water. The measurements show a contact angle around 4° , and one can thereby assume that the AFM silicon tip has a hydrophilic surface. The simple model can also explain why some earlier experiments^{9,20} have not been successful in imaging bubbles in the contact mode, the reason being too large tip angles and less hydrophilic tips.

During force measurements, the gold surface was imaged in the contact mode and areas with nanobubbles were chosen for force measurements. By zooming in, local force measurements were performed in an area with a small number of nanobubbles with diameters ~ 250 nm or less. Hence, these local force measurements give detailed information about interactions with single nanobubbles. Figure 3 shows a typical force measurement obtained in these experiments. We interpret the force curve shown in Figure 3 as the event where a single nanobubble (diameter approximately 150 nm) and the AFM probe tip interact.

In Figure 3, the tip is approaching the surface from right to left. At a tip–sample separation of 12–15 nm, there is a “snap-in”, which represents the event when the tip penetrates the surface of the bubble. The fact that the AFM probe tip is “snapping in” to a tip–sample separation larger than 0 strengthens the hypothesis that an equilibrium can be obtained between the different forces during the scanning of the AFM probe tip over a sample with nanobubbles. Furthermore, the point of snap-in indicates the real height of the nanobubbles, which is larger than

(19) Israelachvili, J. *Intermolecular & Surface Forces*, 3rd ed.; Academic Press: London, 1992.

(20) Mortensen, N. A.; Kühle, A.; Mørch, K. A. *Proceedings of the 3rd Third International Symposium on Cavitation*; Grenoble, France, 1998.

the height measured during contact mode imaging. From the force curve shown in Figure 3, one can deduce that the real height (separation between point 1 and point 3 in Figure 3) of a nanobubble with a diameter ~ 150 nm is 12–15 nm. A region of “soft interaction” where there is forced penetration of the tip into the bubble follows the “snap-in”, until hard-wall contact is made with the gold surface. While the tip is approaching the gold surface during the “soft interaction”, the liquid–solid–gas interface is supposed to move upward along the tip apex. When the tip is pulled back from the surface, another region of “soft interaction” can be observed in the retraction curve. In this situation, the tip has lost contact with the gold surface but it is still in contact with the bubble. At a tip–sample separation of about 15–20 nm, a “snap-out” is observed in the retraction curve and this is the point where the tip and bubble lose contact. Because the tip used in obtaining images in Figure 1 is not the exact same tip as the one used in obtaining the force curve in Figure 3, one cannot compare the forces used quantitatively. However, the force range under which the nanobubbles will be imaged as bright structures according to Figure 3 (during positive force between point 2 and point 3 in the approaching curve) is on the same order of magnitude as the force found from imaging experiments.

Even though the gold surfaces used in the presented results have not been chemically modified to become hydrophobic, contact angle measurement showed that the surfaces had a contact angle around 100° and, thereby, can be considered to be weakly hydrophobic. These unmodified surfaces can be considered to be representative for surfaces normally occurring in many other systems.

Because nanobubbles form spontaneously on these surfaces, they could be the cause of unwanted forces and interactions, and the knowledge of their presence is, therefore, important. It is also important to find methods for avoiding nanobubbles in systems in which they are undesirable. We have carried out preliminary experiments to see if nanobubbles can be removed by rinsing gold surfaces with ethanol *in situ*. Ethanol was introduced into the liquid cell of the AFM to replace the clean water. Both tapping mode and contact mode imaging was performed, and no nanobubbles could be observed. However, when clean water was introduced into the liquid cell again, nanobubbles reappeared on the gold surface. Hence, nanobubbles seem to be difficult to avoid without chemically modifying either the surface or the liquid.

Conclusions

In conclusion, nanobubbles on ultraflat gold surfaces have been imaged with contact mode AFM in an aqueous environment with standard silicon AFM probes. The apparent dimensions of the nanobubbles on AFM contact mode images depend on the scanning force. AFM contact mode imaging, local force measurements, and analysis of the force balance between the tip and the bubble indicate that a force equilibrium can be obtained between the tip and the bubble when the tip is sufficiently sharp and sufficiently hydrophilic. Nanobubbles seem to be a general, but often overseen, phenomenon causing undesired forces in systems involving surfaces in a liquid environment and AFM artifacts.

LA0352669